

Magnetic Resonance Imaging of the Response of a Mouse Model of Non-Small Cell Lung Cancer to Tyrosine Kinase Inhibitor Treatment

Xiangzhi Zhou,^{1,*} Haihua Bao,¹ Ruqayyah Al-Hashem,¹ Hongbin Ji,² Mitchell Albert,¹ Kwok-Kin Wong,² and Yanping Sun¹

Mutational activation of the gene for epidermal growth factor receptor (*EGFR*) is 1 of the main ways by which this receptor induces non-small cell lung cancers (NSCLC). Variant III *EGFR* (*EGFRvIII*) is a potential therapeutic target in NSCLC treatment because of the high frequency of deletion mutations in this protein. This study used noninvasive magnetic resonance imaging (MRI) to investigate the role of an *EGFRvIII* mutant in lung tumorigenesis and tumor maintenance as well as its response to the *EGFR* small molecule inhibitor erlotinib (Tarceva) on bitransgenic mice. Both spin-echo and gradient-echo sequences with and without cardiac and respiratory gating were performed to image the invasive mouse lung tumor driven by *EGFRvIII* mutation. Tumor volumes were measured based on 2-dimensional axial MRI; 3-dimensional rendering of the images were obtained to demonstrate the spatial location and distribution of the tumor in the lung. The MRI results indicated that the tumor driven by the *EGFRvIII* mutation was generated and maintained in the bitransgenic mice with the use of doxycycline. Tumor monitoring via MRI showed that Erlotinib can significantly inhibit the growth of tumor in vivo. MRI has the ability to image mouse lung tumor with different sequences focusing on tissue contrasts between tumor and surroundings. The MRI approaches in this work can be applied on other antitumor drug treatment evaluation in vivo when appropriate sequences are chosen.

Abbreviations: *EGFR*, epidermal growth factor receptor; GEFI, gradient-echo fast imaging; MRI, magnetic resonance imaging; NSCLC, non-small cell lung cancer; *EGFRvIII*, variant III *EGFR*; RARE, rapid acquisition relaxation-enhanced;

Epidermal growth factor receptor (*EGFR*) plays an important role in cell growth in non-small cell lung cancers (NSCLC). This tyrosine kinase receptor induces cellular proliferation leading to cancer through 3 main mechanisms: overexpression of *EGFR* ligands, amplification of *EGFR*, and mutational activation of *EGFR*.²³

Deletions of the extracellular domain are the most frequent *EGFR* mutations among tumor types.¹⁶ These deletions have an activating effect on the receptor, giving cells expressing these truncated receptors a proliferative advantage. The most common truncated receptor is the variant III *EGFR* deletion mutant (*EGFRvIII*, $\Delta 801EGFR$, $\text{del}2\text{-}7EGFR$), which contains an inframe deletion of exons 2 through 7 (801 bp) from the extracellular domain.

The incidence of *EGFRvIII* expression in NSCLC increased when a new monoclonal antibody specific for this variant receptor was used for its immunohistochemical detection.¹⁵ The sustained activation of *EGFRvIII* is implicated in the pathogenesis of NSCLC and thus *EGFRvIII* is a potential therapeutic target in NSCLC treatment.

Currently, 2 main anti*EGFR* agents are used in the preclinical or clinical setting: anti*EGFR* antibodies and small-molecule *EGFR* tyrosine kinase inhibitors.¹⁴ These 2 types of agents have differ-

ent binding points: antibodies bind to the extracellular domain of *EGFR* and block activation of *EGFR* downstream signaling, whereas *EGFR* tyrosine kinase inhibitors bind to the intracellular catalytic domain of the *EGFR* tyrosine kinase, an enzyme that is part of the *EGFR* receptor, by competing with ATP. The tyrosine kinase inhibitor erlotinib (Tarceva) blocks tumor cell growth by targeting the *EGFR* protein and inhibiting *EGFR* signaling. Specifically, erlotinib targets tyrosine kinase and has been shown to produce stasis or regression of tumor growth in human cancer xenograft models, including NSCLC models. Recent studies indicate that erlotinib inhibits the *EGFRvIII* mutant at concentrations higher than those required for inhibition of wild-type receptor.^{10,19}

Magnetic resonance imaging (MRI) is a powerful tool to evaluate malignant tissues and organs, but imaging the lungs by using this technique is challenging due to the fact that almost 80% of the pulmonary volume is filled with air. In addition, the magnetic susceptibility of lung tissue is very different from that of air, and this difference makes the proton T2* in lung tissue shorter and results in a very low signal intensity. Back-projection MRI⁷ yields signal from lung tissues, but the technique is time-consuming because Nyquist sampling at the edge of k-space requires an angularly over-sampled number of spokes, (there are more points sampled in the center than the edge of the k-space), and the image signal-to-noise ratio is not satisfactory.

The use of hyperpolarized gas (³He and ¹²⁹Xe) in MRI is a novel and alternative way to image lung, but ³He MRI can image only regions to which the gas has distributed. The lack of ventilation in

Received: 1 Nov 2007. Revision requested: 29 Nov 2007. Accepted: 18 March 2008.

¹Department of Radiology, Brigham and Women's Hospital, Boston MA; ²Department of Medical Oncology, Dana Farber Cancer Institute, Boston, MA

*Corresponding author. Email: xiazhou@bwh.harvard.edu

lung tumors makes it possible to estimate tumor location and size, but other ventilation obstructions might appear as well. In addition, airway constrictions may block the gas from reaching certain parts of the lung. ^{129}Xe is soluble in blood and tissue, which makes this gas a potential agent to identify not only ventilation obstructions but also blood vessels and tumors.^{1,11} However, this method needs further development to enhance signal intensity because of the low polarization of xenon gas and low xenon concentrations in tissues. Other difficulties for lung MRI are motion effects, including respiratory and cardiac motion, but these effects can be minimized by respiratory and cardiac gating. When fast gradient-echo sequences are applied, a single slice can be scanned with increased number of averages to increase the signal-to-noise ratio without gating.^{4,6}

Despite the difficulties of lung MRI, lung tumor can be visualized easily because of its large fractional water content, given that once a malignant tumor reaches a certain size, it has its own blood supply network. Recently 2D and 3D MRI were used to accurately detect mouse pulmonary solitary tumors based on gradient echo and spin-echo sequences, which can distinguish tumor from surrounding tissues or lesions.¹³ Multishot spin-echo echo-planar imaging has been applied to achieve rapid scans of tumor in murine models of lung cancer.²

Here we used a noninvasive MRI method to investigate the role of an *EGFRvIII* mutant in mouse lung tumorigenesis and tumor maintenance as well as its response to EGFR small-molecule inhibitors (for example, erlotinib). In this work, we used a respiratory- and cardiac-gated T1-weighted spin-echo sequence, a respiratory- and cardiac-gated gradient-echo sequence, and a fast gradient-echo sequence without any gating to assess their utility as a supplemental method to monitor the tumor volume change and regression due to treatment with a tyrosine kinase inhibitor in a very invasive mouse model of NSCLC.

Materials and Methods

A transgenic mouse model of doxycycline-inducible NSCLC driven by *EGFRvIII* was used in this study. Lung adenocarcinoma was induced in 17 mice, of which 11 were treated with tyrosine kinase inhibitor. Doxycycline administration was withdrawn in the remaining 6 mice to evaluate whether the doxycycline-induced *EGFRvIII* mutant is essential for lung tumor development and maintenance. All mice were euthanized after completion of the MRI experiments. All mice were housed in a pathogen-free facility (Dana Farber Cancer Institute, Boston, MA) under appropriate temperature and humidity. All animal experiments and housing conditions were approved by the Harvard Medical Area Standing Committee on Animals and Harvard Medical School IACUC.

Animal model. To examine the role of the *EGFRvIII* mutation in lung tumorigenesis and tumor maintenance *in vivo*, the *Tet-op-EGFRvIII*¹² transgenic mouse was generated to provide tetracycline-inducible expression of *EGFRvIII*. The *Tet-op-EGFRvIII* mouse then was crossed with the *CCSP-rtTA* mouse,^{12,17,22} in which the expression of the reverse tetracycline transactivator protein is targeted to lung type II pneumocytes to generate bitransgenic mice.

To induce *EGFRvIII* expression, adult (age, 6 wk) bitransgenic mice ($n = 17$) were provided with fresh drinking water containing 2 mg/ml doxycycline (Sigma, St Louis, MO) and 5% (w/v) sucrose, whereas the control mouse ($n = 1$) received a 5% sucrose solution without doxycycline. Induction of *EGFRvIII* expression was

verified by RT-PCR detection of *EGFRvIII* transcripts from lung RNA and Western blot analysis of phosphorylated EGFRvIII (Y1068), AKT (S473), and extracellular signal-related kinase 1 and 2 (T202 and Y204) in lung lysates from *Tet-op-EGFRvIII/CCSP-rtTA* mice before and 1 wk after doxycycline administration. After receiving doxycycline-treated water continuously for 8 to 16 wk, *Tet-op-EGFRvIII/CCSP-rtTA* mice underwent MRI to determine total tumor burden.

Treatment with EGFR inhibitor. After prolonged doxycycline treatment, *Tet-op-EGFRvIII/CCSP-rtTA* mice were scanned by MRI to verify tumorigenesis. Then erlotinib (Tarceva, Biaffin, Kassel, Germany) was administered orally at 50 mg/kg daily, together with 2 mg ml⁻¹ doxycycline. After treatment for 1, 2, or 4 wk, mice underwent MRI to determine the reduction in tumor volume. Erlotinib was formulated in 0.5% methylcellulose, 0.4% polysorbate 80 and was administered daily by gavage.

MRI. Measurements were obtained by using a 4.7-T horizontal bore system (Bruker Avance, Karlsruhe, Germany) equipped with a 200-mm inner diameter gradient set to a gradient strength of 30 G/cm. All mice were anesthetized with 1.5% to 2% isoflurane in an oxygen-air mixture via nose cone during the *in vivo* MR scan.

A spin-echo (rapid acquisition relaxation-enhanced; RARE)⁹ sequence with a repetition time of 2035 ms and echo time of 10 ms and a gradient-echo fast imaging (GEFI)⁸ sequence using a repetition time of 230.8 ms, echo time of 3.3 ms, and flip angle of 22.5° were used throughout the study. The slice thickness was 1 mm, and the number of slices was 16 to 18, which was sufficient to cover the entire lung so that tumor volume could be measured. The matrix size was 128 × 128, and the field of view was 2.56 × 2.56 cm². Both cardiac and respiratory gating were applied by using the Biospec system (BioTrig, Bruker BioSpin, Karlsruhe, Germany). For optimal results, respiration was limited to 25 to 35 breaths per minute by adjusting the concentration of isoflurane, with 4 to 5 cardiac beats per respiratory cycle. All animals were scanned by using the described settings and parameters.

In addition, a fast gradient-echo sequence (referred to as SNAP^{4,6}) was tested on 2 mice. The sequence uses ultrafast gradient echo, and the parameters were: repetition time, 12 ms; echo time, 2.7 ms; flip angle, 20°; matrix size, 256 × 256; field of view, 2.56 × 2.56 cm²; and slice thickness, 1 mm. Because this sequence uses a very fast gradient echo, it scans a single slice without triggering any gating.

MRI scans using RARE and GEFI sequences were performed on all mice. Both RARE and GEFI sequences can display the tumors' location, size, and shape in both left and right lungs, as well as any invasion to the pleura, cardiac pericardium and hilus of lung. In addition, the RARE sequence can elaborate details within the tumor and provides clear boundaries with normal lung tissue. It also can distinguish tumors from blood vessels, muscle, and heart. The images obtained from GEFI sequence highlight not only tumor but also blood vessels and heart, and it provides high contrast, which makes it easier to distinguish the smaller nodules and tumor spread to peripheral structures. Figure 1 shows the RARE (image A) and GEFI (image B) scans of a same slice from a mouse.

A third image from the same mouse also is displayed in Figure 1 (image C). The SNAP sequence identifies the heart and main blood vessels as bright areas, but the intensities of tumor and muscle are very similar, making it difficult to distinguish them or

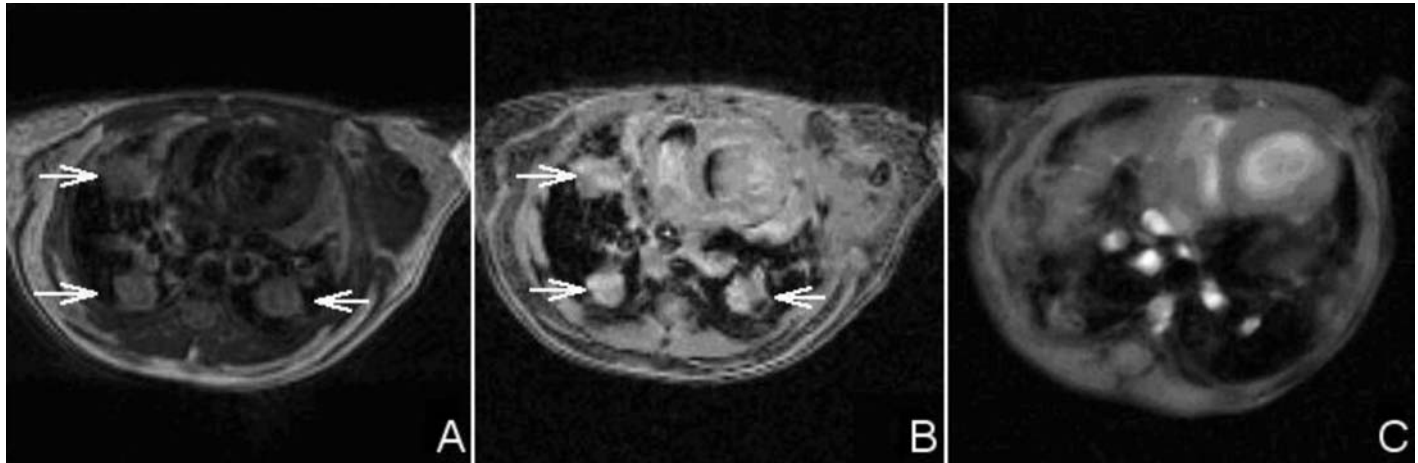


Figure 1. Lung slice images around heart from a mouse with invasive lung tumors. (A) Spin-echo (RARE) image. (B) Gradient-echo (GEFI) image. (C) Fast gradient-echo (SNAP) image. Images A and B are from the same slice, with arrows pointing to tumors; C is from a different slice, in which blood vessels are clearly shown.

to mark the boundary of tumors that attach to the chest wall. The disadvantages of this sequence are obvious: motion effects are still observable; the scan is very time-consuming because only 1 slice is scanned each time; and a large number of averages are required to achieve sufficient a signal-to-noise ratio. In our SNAP experiments, the scan time for a single slice with 40 averages was about 2 min. Although this pulse sequence doesn't require gating, in our experiments, we only used it as a supplemental method to locate the main blood vessels when such information was not available in the images obtained by using the RARE or GEFI sequence.

Measurement and analysis of tumor volume. Volume measurements of the tumors were performed by using inhouse custom software²⁰. Both RARE and GEFI images were registered on the same image stack to locate the tumor and outline the tumor boundary. The tumor volumes for each mouse were averages of 3 separate manual volume measurements by 2 observers (a radiology MD with 7 y clinical experience and a radiology research fellow) from RARE scans. Statistical analysis was performed by using the Student *t* test function in Excel 2003 (Microsoft, Redmond, WA).

Results

MRI of lung relative to doxycycline treatment. Histologic tests (data not shown) confirmed that within 6 to 8 wk of doxycycline administration, *Tet-op-EGFR Δ III/CCSP-rtTA* bitransgenic mice developed atypical adenomatous hyperplasia. Sustained doxycycline induction resulted in the growth of large lung adenomas after 12 wk and adenocarcinomas after 16 wk in these bitransgenic mice.

Withdrawal of doxycycline for 7 d resulted in dramatic tumor regression as revealed by MRI (Figure 2). Interestingly, no tumor regrew even after a 6-wk period of doxycycline withdrawal, indicating that lung tumor maintenance depends on continued expression of *EGFR Δ III*. Therefore, the *EGFR Δ III* mutant is oncogenic in the lung compartment *in vivo* and is essential for lung tumor development and maintenance.

Tyrosine kinase inhibitors treatment on *EGFR Δ III*-driven lung tumors. To evaluate the effects of small-molecule EGFR inhibitors on *EGFR Δ III*-driven lung tumors *in vivo*, *Tet-op-EGFR Δ III/CCSP-*

rtTA, Ink4A/Arf^{-/-} mice were treated with continued doxycycline combined with daily oral administration of vehicle only or erlotinib at 50 mg/kg. Six animals with invasive lung tumors were selected to monitor drug treatment efficacy during a time course. Animals responded to the inhibitor dramatically within 3 wk. Histology (Figure 3) revealed adenocarcinomas before treatment (16 wk after initiation of doxycycline administration) and tumor regression after treatment.

The tumor regression was monitored by MRI, and as expected, the number and size of lung tumors decreased with erlotinib treatment. The detailed tumor changes for typical slices in MRI are given in Figure 4. Figure 4A represents the scan of a mouse prior to inhibitor treatment—nearly half of each lung was covered with tumors. Figure 4B shows the same mouse after 7 d of daily treatment with 50 mg/kg erlotinib and shows a marked decrease in tumor. Animals continued to be treated for an additional 2 wk and were imaged on days 14 and 21 to determine tumor response for the longer drug exposure. Figure 5 displays the tumor volume (mean \pm 1 SD) of the MRI-scanned mice. Initial tumor volume was 369 ± 151 μ l compared with 54 ± 62 μ l 14 d later. Therefore 14 d of erlotinib treatment led to an average reduction of 85.4% in tumor volume in the treated mice.

Three-dimensional rendering of MRI images. To better view the invasion and distribution of tumors in lung, we constructed 3-dimensional images based on 2-dimensional RARE and GEFI images. Tumors location, size, and shape in both left and right lungs, as well as tumor invasion to the pleura, cardiac pericardium, and hilus of lung can clearly be viewed in the 3-dimensional images. The volume-rendered 3-dimensional images again demonstrated the decrease in the number and size of lung tumors after erlotinib treatment, as shown in Figure 6.

Discussion

The MRI results demonstrated that the *EGFR Δ III* mutation-driven tumor was generated and maintained with the presence of doxycycline. The overexpression is switched off by withdrawing doxycycline, causing lung tumor regression. Treatment with small-molecule *EGFR* tyrosine kinase inhibitor caused a dramatic response for mice bearing tumors carrying mutations in *EGFR*

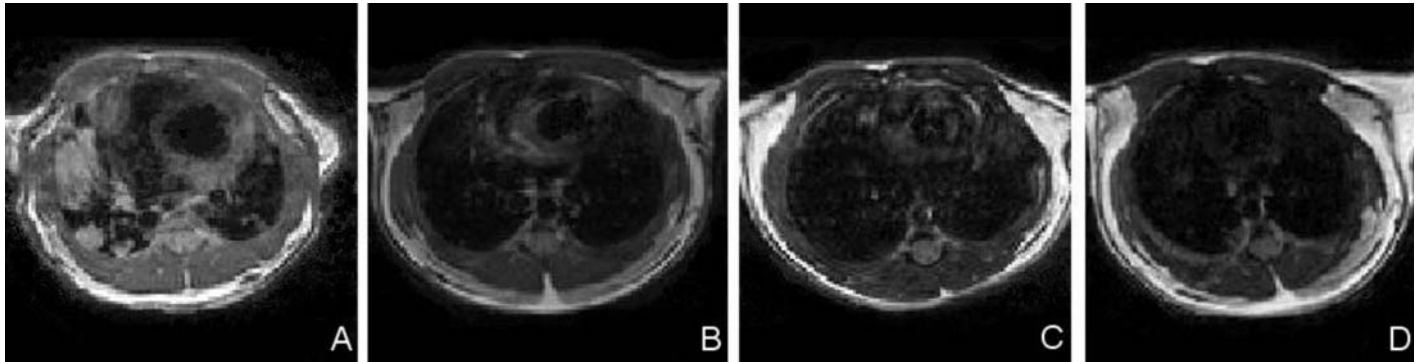


Figure 2. Transverse scans demonstrating the effects of withdrawal after long-term doxycycline administration in a bitransgenic mouse. (A) In a mouse fed with a doxycycline diet for 16 wk, the pleura of the right lung is invaded by tumors in the right lung, and the left lung contains multiple small nodules. (B through D) The effects of doxycycline withdrawal by feeding of a normal diet for (B) 1 wk, (C) 3 wk, and (D) 6 wk, with no observable tumors at the 6-wk point.

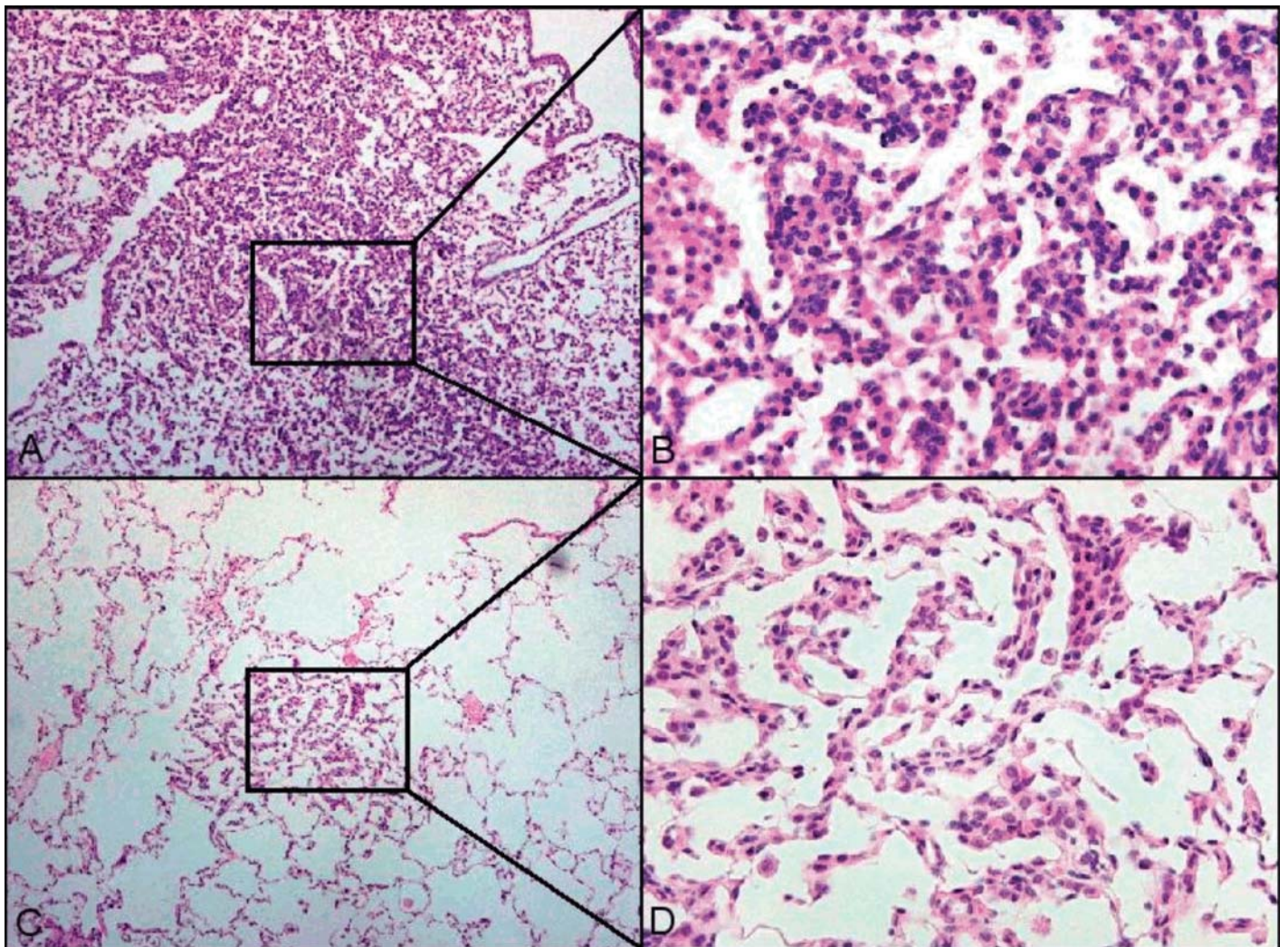


Figure 3. Histology of mouse lung with *EGFRvIII*-driven tumor before and after erlotinib treatment. (A and B) Adenocarcinomas before treatment; (C and D) tumor regression after erlotinib treatment.

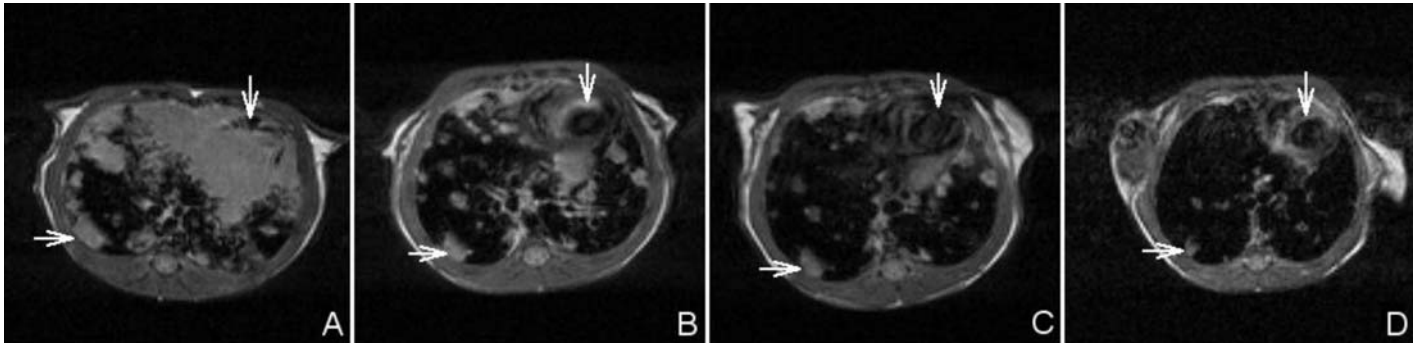


Figure 4. Transverse sections through the thorax of a bitransgenic mouse at various days of erlotinib treatment. (A) Before treatment. (B through D) After treatment for (B) 1 wk, (C) 2 wk, and (D) 4 wk. Notice the regression of the 3 nodules in right lung. Vertical arrows indicate the heart; horizontal arrows indicate examples of tumor nodules.

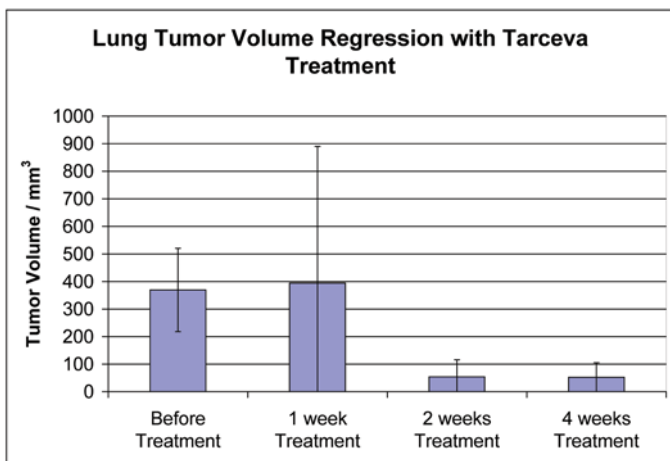


Figure 5. Lung tumor volume before and after 1, 2, and 4 wk of treatment with a tyrosine kinase inhibitor. Compared with tumor volume before treatment, tumor regression was significant after 2 wk ($P = 0.047$) and 4 wk ($P = 0.017$) of treatment.

kinase domains. Tumor monitoring by MRI showed that erlotinib can inhibit tumor growth in vivo due to inhibition of the growth of cells harboring *EGFRvIII* mutations.

Erlotinib is a reversible EGFR inhibitor to which patients with NSCLC eventually develop resistance.³ Two mice undergoing erlotinib treatment had obvious tumor regeneration within 4 wk continuous treatment, and this tumor volume fluctuation during long-term drug administration may indicate the reversible bind-

ing property of erlotinib. Reportedly the irreversible inhibitor HKI-272 covalently binds to the *EGFR* kinase domain cleft and can overcome resistance,^{18,21} thus suggesting that HKI-272 may be more effective for treating cancers that harbor the *EGFRvIII* mutation.

In this work, noninvasive mouse lung tumor monitoring was accomplished by using 2-dimensional MRI with and without cardiac and respiratory gating. Spin-echo (RARE), gradient-echo (GEFI), and fast gradient-echo (SNAP) sequences were implemented to scan the entire lung for tumor volume measurements. However, the contrast between tumor and surroundings can vary under different sequences (see Figure 1).

Other lesions frequently coexist with tumor during the development of lung carcinoma, and some of these additional lesions can have similar signal intensity as tumor in MRI scans. Inflammation-related lesions such as consolidation, pleuritis, and peribronchial vascular inflammation may complicate the identification of tumor, but they can be ruled out by histopathology. Atelectasis can be identified in MRI scan by its relatively lower signal intensity, which can be further proved by histology testing after treatment. However, in our study, 16 wk of continuous doxycycline administration ensured that all the mice developed diffuse adenocarcinoma; MRI did not reveal any complicating lesions; and histopathology checks confirmed that the dominant lesion was tumor.

In conclusion, the present work demonstrates volume variation in *EGFRvIII* mutation-driven lung tumor as evaluated by both spin-echo and gradient-echo sequences. Combining sequences to identify tumor and to simplify its complexity is important in



Figure 6. Three-dimensional renderings of lung and tumor volumes from 2-dimensional MRI slices of a bitransgenic mouse. (A) Before treatment and after (B) 1 wk, (C) 2 wk, and (D) 4 wk of treatment with erlotinib. Blue areas indicate tumors.

mouse MRI, because a single sequence is inadequate to collect sufficient information in complicated cases.

Acknowledgment

This work was supported in part by a grant (Contract ID 50203501) from the Swedish Research Council (to XZ).

References

1. **Albert MS, Balamore D.** 1998. Development of hyperpolarized noble gas MRI. *Nucl Instrum Methods Phys Res A* **402**:441–453.
2. **Bankson JA, Ji L, Ravoori M, Han L, Kundra V.** 2008. Echo-planar imaging for MRI evaluation of intrathoracic tumors in murine models of lung cancer. *J Magn Reson Imaging* **27**:57–62.
3. **Baselga J.** 2006. Targeting tyrosine kinases in cancer: the second wave. *Science* **312**:1175–1178.
4. **Beckmann N, Tigani B, EkatoDRAMIS D, Borer R, Mazzoni L, Fozard JR.** 2001. Pulmonary edema induced by allergen challenge in the rat: noninvasive assessment by magnetic resonance imaging. *Magn Reson Med* **45**:88–95.
5. **Beckmann N, Tigani B, Sugar R, Jackson AD, Jones G, Mazzoni L, Fozard JR.** 2002. Noninvasive detection of endotoxin-induced mucus hypersecretion in rat lung by MRI. *Am J Physiol Lung Cell Mol Physiol* **283**:L22–L30.
6. **Frahm J, Haase A, Matthaei D.** 1986. Rapid NMR imaging of dynamic process using the FLASH technique. *Magn Reson Med* **3**:321–327.
7. **Gewalt SL, Glover GH, Hedlund LW, Cofer GP, MacFall JR, Johnson GA.** 1993. MR microscopy of the rat lung using projection reconstruction. *Magn Reson Med* **29**:99–106.
8. **Haase A, Frahm J, Matthaei D, Hanicke W, Merboldt K-D.** 1986. FLASH imaging: rapid NMR imaging using low flip-angle pulses. *J Magn Reson* **67**:258–266.
9. **Hennig J, Nauerth A, Friedburg H.** 1986. RARE imaging: a fast imaging method for clinical MR. *Magn Reson Med* **3**:823–833.
10. **Hidalgo M.** 2003. Erlotinib: preclinical investigations. *Oncology (Williston Park)* **17 Suppl 12**:11–16.
11. **Ireland RH, Bragg CM, McJury M, Woodhouse N, Fische S, van Beek EJ, Wild JM, Hatton MQ.** 2007. Feasibility of image registration and intensity-modulated radiotherapy planning with hyperpolarized helium-3 magnetic resonance imaging for non-small-cell lung cancer. *Int J Radiat Oncol Biol Phys* **68**:273–281.
12. **Ji H, Zhao X, Yuza Y, Shimamura T, Li D, Protopopov A, Jung BL, McNamara K, Xia H, Glatt KA, Thomas RK, Sasaki H, Horner JW, Eck M, Mitchell A, Sun Y, Al-Hashem R, Bronson RT, Rabindran SK, Discafani CM, Maher E, Shapiro GI, Meyerson M, Wong KK.** 2006. Epidermal growth factor receptor variant III mutations in lung tumorigenesis and sensitivity to tyrosine kinase inhibitors. *Proc Natl Acad Sci USA* **103**:7817–7822.
13. **Kubo S, Levantini E, Kobayashi S, Kocher O, Halmos B, Tenen DG, Takahashi M.** 2006. Three-dimensional magnetic resonance microscopy of pulmonary solitary tumors in transgenic mice. *Magn Reson Med* **56**:698–703.
14. **Mendelsohn J, Baselga J.** 2006. Epidermal growth factor receptor targeting in cancer. *Semin Oncol* **33**:369–385.
15. **Okamoto I, Kenyon LC, Emler DR, Mori T, Sasaki J, Hirosako S, Ichikawa Y, Kishi H, Godwin AK, Yoshioka M, Suga M, Matsumoto M, Wong AJ.** 2003. Expression of constitutively activated EGFRvIII in non-small cell lung cancer. *Cancer Sci* **94**:50–56.
16. **Paez JG, Jänne PA, Lee JC, Tracy S, Greulich H, Gabriel S, Herman P, Kaye FJ, Lindeman N, Boggon TJ, Naoki et al.** 2004. EGFR mutations in lung cancer: correlation with clinical response to gefitinib therapy. *Science* **304**:1497–1500.
17. **Perl AK, Tichelaar JW, Whitsett JA.** 2002. Conditional gene expression in the respiratory epithelium of the mouse. *Transgenic Res* **11**:21–29.
18. **Rabindran SK, Discafani CM, Rosfjord EC, Baxter M, Floyd MB, Golas J, Hallett WA, Johnson BD, Nilakantan R, Overbeek E, Reich MF, Shen R, Shi X, Tsou HR, Wang YF, Wissner A.** 2004. Antitumor activity of HKI-272, an orally active, irreversible inhibitor of the HER-2 tyrosine kinase. *Cancer Res* **64**:3958–3965.
19. **Rosell R, Taron M, Reguart N, Isla D, Moran T.** 2006. Epidermal growth factor receptor activation: how exon 19 and 21 mutations changed our understanding of the pathway. *Clin Cancer Res* **12**:7222–7231.
20. **Schmidt KF, Ziu M, Schmidt NO, Vaghiasa P, Cargioli TG, Doshi S, Albert MS, Black PM, Carroll RS, Sun Y.** 2004. Volume reconstruction techniques improve the correlation between histological and in vivo tumor volume measurements in mouse models of human gliomas. *J Neurooncol* **68**:207–215.
21. **Sequist LV.** 2007. Second-generation epidermal growth factor receptor tyrosine kinase inhibitors in non-small cell lung cancer. *Oncologist* **12**:325–330.
22. **Tichelaar JW, Lu W, Whitsett JA.** 2000. Conditional expression of fibroblast growth factor 7 in the developing and mature lung. *J Biol Chem* **275**:11858–11864.
23. **William Pao, Miller VA.** 2005. Epidermal growth factor receptor mutations, small-molecule kinase inhibitors, and non small-cell lung cancer: current knowledge and future directions. *J Clin Oncol* **23**:2556–2568.